Cancer-associated hypersialylated MUC1 drives the differentiation of monocytes into macrophages with a pathogenic phenotype

Richard Beatson[1], Rosalind Graham[1], Fabio Grundland Freile[1], Domenico Cozzetto[2], Shichina Kannambath[3], Ester Pfeifer[1], Natalie Woodman[4], Julie Owen[4], Rosamond Nuamah[3], Ulla Mandel[5], Sarah Pinder[6], Cheryl Gillett[4], Thomas Noll[7], Ihssane Bouybayoune[6], Joyce Taylor-Papadimitriou[1], Joy M. Burchell[1].

[1]Breast Cancer Biology, [4]KHP Tissue Bank, [6]Breast Pathology, Comprehensive Cancer Centre, King's College London, Guy's Cancer Centre, Guy's Hospital, London SE1 9RT. UK

[2]Translational Bioinformatics, [3]Genomics Facility, National Institute for Health Research Biomedical Research Centre at Guy's and St Thomas' NHS Foundation Trust and King's College London, London, SE1 9RT, UK

[5]Copenhagen Centre for Glycomics, Departments of Cellular and Molecular Medicine and Odontology, Faculty of Health Sciences, University of Copenhagen, Blegdamsvej 3, 2200 N Copenhagen, Denmark.

[7]Cell Culture Technology, Faculty of Technology & CeBiTec, Bielefeld University, P.O. Box 10 01 31, 33501 Bielefeld, Germany

Abstract

The tumour microenvironment plays a crucial role in the growth and progression of cancer and the presence of tumour-associated macrophages (TAMs) is associated with poor prognosis. Recent studies show that TAMs show transcriptomic, phenotypic, functional and geographical diversity. Here we show that a sialylated tumour-associated glycoform of the mucin MUC1, MUC1-ST, through the engagement of Siglec-9 can specifically and independently induce the differentiation of monocytes into TAMs with a unique phenotype. These TAMs can recruit and maintain neutrophils, inhibit the function of T cells, degrade

basement membrane allowing for invasion, are inefficient at phagocytosis, and can induce plasma clotting. This novel macrophage phenotype is enriched in the stroma at the edge of breast cancer nests and their presence is associated with poor prognosis in breast cancer patients.

Introduction

The tumour metropolis consists of an ecosystem of tumour cells, stroma and infiltrating immune cells, and in breast cancers the tumour microenvironment (TME) can form 50% of the tumour mass. Tumour-associated macrophages (TAMs) make a considerable contribution to the TME and are associated with poor prognosis as demonstrated by a recent meta-analysis of sixteen studies in breast cancer [1]. TAMs contribute to all stages of cancer progression through a variety of mechanisms including promoting angiogenesis, inducing immune suppression and promoting inflammation [2,3]. Indeed, their importance in the initiation of mammary tumours has been shown by inducing premature recruitment of macrophages into the mammary gland which results in the promotion of malignancy [4], whereas depletion of macrophages can completely inhibit the growth of transplantable tumours [5].

In health, the majority of tissue resident macrophages are believed to originate from the erythroid-myeloid progenitors in the yolk sac while most macrophages present in tumours are recruited from circulating monocytes [6]. Historically macrophages have been divided into M1-like which are pro-inflammatory and anti-tumour and M2-like which are involved in wound healing and thought to promote tumour growth. However, it is clear that this binary classification is no longer valid as data coming from RNAseq and single cell RNAseq show transcriptional diversity and M1 and M2 defining genes expressed by the same cell [7,8,9]. Indeed, TAMs are phenotypically plastic and factors produced by the cancer cells and the TME can induce macrophages to become tumour-promoting. These can include factors secreted by the tumour cells such as chemokines, cytokines and metabolites secreted and consumed within the TME [10].

Changes in glycosylation are common features of malignancy and often result in increased sialylation [11-14]. Members of the Siglec family of sialic acid binding lectins are expressed by many immune cells including monocytes and macrophages [15]. Siglecs are involved in regulation of the immune system and many contain immunoreceptor tyrosine-based inhibitory motifs (ITIMs). Indeed, recent studies have implicated binding of sialic acid to Siglecs as a means of cancer immune evasion [16-18]. Siglec-1 (CD169), which importantly lacks an ITIM, is the most common siglec expressed by macrophages [19] and high expression of *SIGLEC1* together with high expression of *CCL8* was associated with poorer prognosis in breast cancer patients [20].

MUC1 is a surface bound and secreted mucin that is known to be over-expressed, de-polarised and aberrantly O-glycosylated in the majority of breast carcinomas. The alterations in O-glycosylation, from long branched chains to shorter structures, are primarily due a change in glycosyltransferase expression [11-14]. These short glycans are frequently hyper-sialylated and we have shown that sialylation of the short trisaccharide (Neu5Acα2,3Galβ1,3GalNAc) known as sialylated T (ST) leads to increased tumour growth in mouse models [21] and that this increased growth is immune cell dependent [22]. Moreover, MUC1 carrying the ST glycan is the dominant MUC1 glycoform found in sera of cancer patients [23]. Although the aberrant glycosylation resulting in MUC1 carrying the ST glycan has been known for many years and the conservation and high prevalence of this glycoform in breast and other adenocarcinomas suggested functionality, the mechanisms involved in its association with tumour progression have been poorly understood.

We and others have shown that MUC1 can bind to Siglec-9 [24,25] that is expressed by monocytes, macrophages and some T cells [15,26]. We found that the sialylated tumour associated glycoform of MUC1, MUC1-ST, bound to Siglec-9 expressed by monocytes and induced monocytes to secrete factors associated with tumour progression [24]. Here we show that MUC1-ST is expressed by the majority of breast cancers and, acting in serum-free medium without the addition of cytokines, has the ability to induce the differentiation of monocytes to macrophages and to maintain their viability. These macrophages show

functional characteristics of TAMs, including potent basement membrane disruption, and can be identified in a specific region of primary breast cancers known to be associated with a worse prognosis. The transcriptional profile of these MUC1-ST macrophages reveals a novel phenotype with multiple upregulated factors associated with poor prognosis, and defines a signature associated with poor survival of breast cancer patients.

Results

The ST glycoform of MUC1 is very common in breast cancers and correlates with stromal macrophage infiltrate.

Analysis of 53 whole primary breast cancers showed that a sialylated glycoform of MUC1, MUC1-ST (which carries the glycan, Neu5Acα2,3Galβ1,3GalNAc), was expressed by 83% of breast cancers (figure 1a and b). Analysis of the breast cancer subtypes showed that triple negative breast cancers (TNBC) had the lowest expression of MUC1-ST and Oestrogen Receptor (ER) positive breast cancers the highest (figure S1a). Given the high expression of MUC1-ST in breast cancers, the well-established impact of macrophage presence, and that MUC1-ST can bind to Siglec-9 expressed by macrophages [24], we analysed cases for macrophage infiltrate and assessed for any association with MUC1-ST.

Initially we documented the location of CD163+ macrophages, finding a higher number of macrophages on the edge of the tumour nests (figure 1c, S1b). Figure 1d shows examples of two cases with high and low expression of MUC1-ST and the staining of consecutive sections by IHC of CD163. Scoring of macrophages in different geographical regions by manual (figure 1e) and automated (figure S1c) methodologies revealed a significant association between MUC1-ST and CD163 on the edge of the tumour nests. With there being no correlation between MUC1-ST and tumour derived CSF1 (figure S1d), we hypothesised that MUC1-ST itself may be able to drive macrophage differentiation in this specific location.

MUC1-ST alone can induce primary healthy monocytes to differentiate into macrophages with a TAM like phenotype.

Given the findings in figure 1 and the fact that MUC1-ST can bind to and activate monocytes [24], we assessed whether MUC1-ST alone could drive the differentiation of monocytes into macrophages. Monocytes isolated from the PBMCs of healthy donors were treated with MUC1-ST, MUC1-ST treated with sialidase to remove the sialic acid (MUC1-T) or M-CSF as a control, all in serum-free medium for 7 days. Figure 2a and 2b show that MUC1-ST supported the viability of macrophages similar to M-CSF but this was not observed when the sialic acid was removed from the MUC1-ST (MUC1-T). Phenotypic analysis showed that MUC1-ST treated monocytes expressed TAM-like markers, showing significantly higher levels of PD-L1 and CD206 than M-CSF treated monocytes or monocytes treated with MUC1-T and so lacking sialic acid (figure 2c). MUC1-ST treated monocytes also showed expression of CD163 and low levels of CD86 (figure 2c). Moreover, the induction of this phenotype by MUC1-ST was dose dependent (figure S2a).

Given that treatment of monocytes with MUC1-ST can induce the secretion of M-CSF (figure S2b), monocytes were cultured with M-CSF or MUC1-ST in the presence of an M-CSF neutralising antibody or isotype control. While there was a total lack of viable cells when monocytes were cultured with M-CSF in the presence of the M-CSF neutralising antibody, this antibody had no effect on the viability of MUC1-ST culture cells, nor on their phenotype (figure 2d and 2e). This shows that factors other than M-CSF were supporting the differentiation and viability of the MUC1-ST macrophages.

The transcriptome of MUC1-ST induced macrophages is significantly different to M-CSF induced macrophages.

As MUC1-ST supported the differentiation of monocytes to TAM-like macrophages, this glycoform is commonly expressed in breast cancers and correlated with macrophages present in the stroma around the cancer nests, we wished to further explore the relationship between MUC1-ST and TAMS. RNAseq was performed on MUC1-ST induced macrophages and compared to donor matched M-CSF induced macrophages. Monocytes from three healthy donors were treated with M-CSF or MUC1-ST for 7 days in serum free medium, viable cells

sorted, the RNA isolated, and RNAseq performed. The expressed genes are documented in table 1. Application of CIBERSORT [27] analysis to the starting monocytes and the MUC1-ST or M-CSF induced macrophages confirmed the monocyte-derived macrophage immune subtype of the MUC1-ST induced cells as M0-like (figure S3a). Figure 3a and 3b show the hierarchical clustering and t-sne plots of the samples, and figure 3c the volcano plots of the transcripts after differential analysis comparing matched MUC1-ST macrophages and M-CSF macrophages. These data illustrate that M-CSF and MUC1-ST induced macrophages express a very different profile of genes. Also shown are the top and bottom 50 genes differentially expressed by MUC1-ST macrophages (figure 3d and 3e). Two of the most highly differentially expressed genes in the MUC1-ST macrophages were *CXCL5* and *SERPINE1*/PAI-1 (figure 3f) and the validation of the expression of these mRNAs at the protein level is shown in figure 3g. Importantly, the expression of CXCL5 by MUC1-ST induced macrophages was significantly reduced when MUC1-ST was stripped of its sialic acid (figure 3h) and the expression was also significantly inhibited by a Siglec-9 antibody (figure 3i). The expression of PAI-1 also showed similar trends. Moreover, when monocytes were co-cultured with the breast cancer line T47D that carries the MUC1-ST glycoform [28], CXCL5 was secreted by the myeloid cells and was significantly reduced when the T47D cells were treated with sialidase to remove the sialic acid (figure 3j). Furthermore, monocytes cultured in the presence of T47D cells that had been engineered so that MUC1 carries long, branched chains rather than ST [28] showed a reduction in the secretion of CXCL5 (figure 3k). Further evidence for the requirement of sialic acid on MUC1-ST is shown in figure S3 where a further three validated genes (figure S3b,c) showed reduced expression when sialic acid is removed from MUC1-ST (figure S3d). Furthermore, the addition of a Siglec-9 antibody during the differentiation also reduces the expression of these three proteins (figure S3e). Figure S3f shows that the expression of a further 17 genes, including PD-L1 which was highly significantly upregulated in MUC1-ST macrophages, and 15 of these were validated at the protein level. Taken together these data suggest that MUC1-ST binding to Siglec-9 is responsible for the profile of gene expression observed in MUC1-ST induced macrophages.

MUC1-ST induced macrophages have distinct functional capabilities.

Neutrophil function. Neutrophils have been shown to contribute to breast cancer metastasis [29-31]. A number of chemokines such as CXCL5, CXCL8 and CCL24 [32,33] that are differentially expressed in MUC1-ST macrophages compared to M-CSF macrophages are involved in neutrophil recruitment (figure 4a). Leukotrienes also have a chemotactic effect on neutrophils [34] and ALOX5 which catalyses the first step in leukotriene synthesis is also upregulated in MUC1-ST macrophages compared to M-CSF induced macrophages (figure 4a). Therefore, neutrophils isolated from healthy donors were cultured in the supernatant from MUC1-ST induced macrophages or M-CSF macrophages. MUC1-ST macrophage supernatant was able to maintain the viability of 72% of the neutrophils at 48h in comparison to M-CSF macrophage supernatant that was no better than medium alone (figure 4b and 4c). Moreover, the expression of CD15, which is the Lewis^x glycan that mediates neutrophil adhesion to dendritic cells and is associated with neutrophil maturation [35], was elevated on neutrophils incubated with supernatant from MUC1-ST induced macrophages (figure 4c). Supernatant from MUC1-ST induced macrophages also significantly increased the migration of neutrophils compared to M-CSF macrophage supernatant (figure 4d).

Invasion. Given that MUC1-ST induced macrophages expressed genes associated with extracellular matrix disassembly, particularly MMP14 the expression of which is dependent on the sialic acid carried on MUC1-ST (figure 4e and 4f), and given the reported importance of macrophage mediated basement membrane degradation in promoting invasion and metastasis [36,37], the invasion of neutrophils through basement membrane extract towards the various supernatants was investigated. Figure 4g shows that while control media and M-CSF induced macrophage medium induced no invasion of neutrophils, supernatant from MUC1-ST macrophages induced a significant number of cells to invade through basement membrane within 2 hours. Moreover, supernatant from MUC1-ST induced macrophages induced the invasion through the basement membrane of the breast cancer cell line, MCF-7, in a similar manner (figure 4h).

Clotting. Cancer patients are at a higher risk than the general population of developing serious bloods clots and breast cancer patients are at a risk of developing venous thromboembolism [38]. Two genes associated with blood coagulation, coding for factor 8 (*F8*) and tissue factor (*F3*) were also found to be differentially expressed by MUC1-ST induced macrophages (figure 5a). Therefore, the expression of tissue factor by MUC1-ST and M-CSF induced macrophages was investigated. While there was no difference in the surface expression of tissue factor between MUC1-ST and M-CSF induced macrophages (figure 5b), MUC1-ST macrophages secreted significantly more tissue factor than M-CSF macrophages and there was a requirement for sialic acid (figure 5c). Moreover, supernatant from MUC1-ST macrophages induced significantly faster clotting than M-CSF macrophage supernatant (figure 5d).

Phagocytosis. A number of genes associated with phagocytosis (e.g. CD36) were significantly downregulated in MUC1-ST induced macrophages although the expression of some scavenger receptor genes such as MARCO which has been associated with a poor prognosis in breast cancer [39] were significantly upregulated (figure S3f, table 1). The phagocytic ability of the MUC1-ST induced macrophages was therefore investigated. Figure 5e and 5f, show that MUC1-ST macrophages were significantly less efficient at phagocytosis compared to M-CSF macrophages of both dextran (figure 5e) and a breast cancer cell line compared to M-CSF macrophages (figure 5f, figure S4a).

T cell function. Genes associated with the inhibition of T cell function such as PD-L1 and IDO and protein expression of arginase were upregulated in MUC1-ST macrophages whereas CD86 was downregulated (table 1, figure S3, S4b). We therefore investigated the ability of MUC1-ST macrophages to inhibit T cell proliferation. Indeed, supernatant from MUC1-ST monocytes significantly reduced the proliferation and viability of anti-CD3 stimulated PBMC and the proliferation and viability of PBMC in a mixed lymphocyte reaction (figure 5g,h, figure S4c).

Taken together these data indicate that macrophages induced by MUC1-ST show functional characteristics of TAMs, in that they recruit and maintain neutrophils, degrade basement membrane, are inefficient at phagocytosis and inhibit T cell proliferation and viability. Moreover, these macrophages can promote blood clotting.

MUC1-ST induced macrophages are present in primary breast cancer and associated with poor prognosis.

To investigate the presence of MUC1-ST induced macrophages in primary breast cancer, the expression of *SERPINE1* (PAI-1) which is differentially expressed by MUC1-ST macrophages (figure 3f and 3g) was measured by RNAscope on consecutive sections. Figure 6a and 6b show that *SERPINE1* is upregulated in breast cancer and that significantly higher expression is found in the stroma around the edges of the nests of cancer cells compared to within the cancer cell nests or the stroma around the tumour (figure 6b). Moreover, *SERPINE1* expression in cells found in the stroma around the edges of the cancer cell nests is significantly correlated with MUC1-ST expression (figure 6c).

In addition, 24 primary breast cancers were double stained for CD68 and CXCL5 (figure 6d). Importantly, CD68 macrophages expressing CXCL5 were found within the cancers and with significantly higher numbers in the stroma around the nests of cancer cells (figure S5a). Moreover, there was a trend that $CD68^{+}CXCL5^{+}$ macrophages in the stroma around the edges of the cancer nests to be associated with MUC1-ST expression (figure 6e).

To ascertain whether the cells we were observing in situ expressed SIGLEC9, we adopted two approaches: 1) Analysis of the TCGA breast cancer database shows a highly significant correlation between CD163 or CD68 and SIGLEC9 but not with the epithelial markers, EPCAM or KRT8 (figure S5b). 2) BASEscope analysis of our cohort of breast cancer showed expression of SIGLEC9 within the stroma, edge and nest of the tumour (figure S5c) in a similar manner to CD163 staining. Encouragingly, SIGLEC9 expression showed a trend for an inverse correlation with MUC1-ST expression suggesting the down regulation of the receptor

upon engagement (figure S5d), which was also observed at both the RNA and protein level in our in vitro studies (figure S3f).

Finally, to determine whether these proteins may be present in the TME, we assessed for seven top validated factors, and MUC1, in the interstitial fluid of fresh breast cancers (figure S5e), finding all factors, to varying levels, in all tumours tested.

As MUC1-ST macrophages were able to recruit and maintain neutrophils, inhibit T cell responses and enable cellular invasion through basement membrane extract, we investigated if MUC1-ST expression or MUC1-ST macrophage presence were associated with poor prognosis in breast cancers. Firstly, determining the expression of the top ten prognostic genes associated with a poor or favourable prognosis in all cancers identified by Gentles et al. [27], we showed that 8 out of 10 genes associated with poor prognosis were upregulated by MUC1-ST macrophages compared to M-CSF macrophages (figure 7a). In contrast, four of the genes associated with a good prognosis were differentially upregulated by M-CSF induced macrophages (figure 7b). Secondly, we had data on lymph node involvement for 20 patients in our cohort, and we observed a significant correlation between the percentage of involved lymph nodes and the expression of MUC1-ST (figure 7c). Finally, we assessed whether a MUC1-ST macrophage gene signature consisting of the top nine differentially expressed genes was associated with clinical outcome using the TCGA database. Figure 7d shows a highly significant correlation between a high MUC1-ST macrophage signature and shorter disease-free and overall survival.

Discussion

Aberrant glycosylation, often resulting in hypersialylation is a common feature of cancer [11-14] and this has been shown to lead to the engagement of Siglecs [16-18,24,25]. The MUC1 mucin which carries multiple O-linked glycans shows a dramatic change in glycosylated in many cancers, including breast cancers, resulting in the core protein carrying multiple sialylated tri-saccharides known as ST. Here we have shown that MUC1-ST in serum-free medium and in

the absence any other factor can induce monocytes to differentiate into macrophages with a unique phenotype that has not previously been described. The requirement for sialic acid on MUC1 and the data using a Siglec-9 antibody to block the interaction, indicate that MUC1-ST macrophages are induced through the engagement of Siglec-9 expressed by monocytes. Previous data have shown that when MUC1-ST binds to Siglec-9, phosphorylation of Siglec-9 is reduced, evoking calcium flux and activation of the MEK-ERK pathway [24].

We applied CIBERSORT [27] to the transcriptome of these MUC1-ST induced macrophages and confirmed their macrophage phenotype, we then validated 22/24 differential hits. These macrophages generated *in vitro* showed the functional characteristics of TAMs in that they are inefficient at phagocytosis, inhibit T cell proliferation, recruit neutrophils and promote invasion. Analysis of 53 breast cancers demonstrated the presence of this macrophage subtype in primary breast cancers and using the top nine differentially expressed genes by the MUC1-ST macrophages, we showed a significant association with poor prognosis. Our data indicate that at least one of the mechanisms whereby MUC1-ST can affect progression of cancers is by the direct induction of monocyte differentiation into macrophages with a TAM-like phenotype without the need for any additional factor**.**

The presence of TAMs being pro-tumoral is now well established in breast cancer, and a meta-analysis of 16 studies demonstrated that high density of TAMs is associated with a poor prognosis [1]. Moreover, the specific location of TAMs within a tumour is known to have an impact on their pro-tumour activity. It is the TAMs outside the nests in the stroma rather than within the nest of the cancer cells that are associated with the worst outcome. Indeed, CD163 or CD68 macrophages in the stroma rather than in the cancer cell nests have been shown to correlate with a poor prognosis [40,41]. Furthermore, Richardson et al. [41] report that stromal cells expressing M-CSF, also expressed by MUC1-ST macrophages, are associated with metastasis. Importantly we found a correlation between the intensity of MUC1-ST staining of the cancer cells and CD163+ macrophages in the stroma around the nests of cancer cells. Moreover, macrophages with a MUC1-ST induced phenotype, demonstrated by expression

of CXCL5 and *SERPINE1* found in the stroma around the edge of the nests, correlated with MUC1-ST expression. These data suggest that MUC1-ST is driving the generation of these specific TAMs in this specific location.

Historically TAMs within human breast cancer had been identified only by immune histochemistry. However, recently macrophages isolated from breast cancers have been analysis by RNAseq [7], CyTOF [42] and single cell RNAseq [8]. The Pollard lab identified a TAM signature also associated with poor prognosis and that is enriched in HER2 positive breast cancers. One of the identified genes was *SIGLEC1*, which when translated engages with CCL8 in a tumour cell regulatory loop [20]. This TAM type is different to the one we have identified as *SIGLEC1 and CCL8* were two of the most highly down-regulated genes in the MUC1-ST macrophages (table 1). Interestingly, Siglec-1+ macrophages within the regional lymph nodes of patients have also been associated with good prognosis in breast cancers [43] and, functionally, have been shown to inhibit Treg expansion in mice [44], suggesting different roles in different locations. Comparative and correlative analysis of the transcripts expressed by the MUC1-ST induced macrophages suggests that the MUC1-ST macrophage subtype is most closely related to subtype 23 identified by Azizi et al. [8]. Interestingly, the authors determined that the TAMs in cluster 23 were of mixed classical 'M1' and 'M2' signatures, something that is apparent in the phenotype of MUC1-ST macrophages.

MUC1-ST macrophages can produce factors that are able to modulate the immune micro-environment. Firstly, factors such as CXCL5, CXCL8, CCL24, S100A8 [32,33] and ALOX5 [34] expressed by MUC1-ST macrophages are involved in neutrophil recruitment and our *in vitro* data show that MUC1-ST macrophages can indeed induce neutrophil migration and also maintain neutrophil viability. Increased neutrophil numbers in breast cancers is associated with worse survival [30] and the absence of neutrophils profoundly reduces pulmonary metastasis in a murine model of breast cancer [29]. Intriguingly, in this model system it is IL-1β, a cytokine also highly upregulated in the MUC1-ST macrophages that elicits IL-17 expression by $\gamma\delta$T cells resulting in the G-CSF dependent expansion and polarisation of neutrophils [29].

The factors released by the MUC1-ST macrophages and the functional data suggests a very strong relationship between these macrophages and neutrophils. Secondly, MUC1-ST macrophages produce factors including PD-L1 (*CD274*), PD-L2 (*PDCDILG2*), IDO1 and arginase that negatively regulate the activity of T cells, CCL24 which acts to recruit resting T cells but not activated T cells [45], and CCL18 that recruits Tregs [46], whilst also downregulating CD86, important for the co-stimulation of T cells. Interestingly TAMs isolated from breast cancers have previously been seen to secrete large amounts of CCL18 and promote metastasis through CCL18 binding to PITPNM3 [47]. Our *in vitro* studies confirm that MUC1-ST macrophages inhibit the proliferation of T cells and decrease their viability.

The MUC1-ST macrophages show further characteristics of TAMs in that they are inefficient at phagocytosis and induce the invasion of both neutrophils and the minimally invasive breast cancer cell line MCF-7. Interestingly the proteases that are upregulated in the MUC1-ST macrophages are MMP14 and MMP2, while MMP9 and MMP19 are down regulated compared to M-CSF induced macrophages. The inhibitors of MMPs, the TIMPs, also show an interesting trend, with TIMP1 up and TIMP2 down in MUC1-ST macrophages while the expression of TIMP3 is almost completed gone. MMP14 (also known as MTI-MMP) is a membrane bound protease that activates the pro-enzyme form of MMP2 also known as gelatinase A [48]. MMP14 and MMP2 both degrade the extracellular matrix especially collagen IV, found in basement membranes, and indeed MMP14 and MMP2 have been shown to promote cancer invasion and metastasis [49]. Indeed in the same study, MMP14 and MMP2 detection in the non-cancerous cells in breast cancer is associated with poor overall survival, with high MMP2/MMP14 low TIMP2 stromal cells, a similar phenotype to MUC1-ST macrophages, being associated with the poorest outcome [49]. Further to this, MMP14 can also induce HIF transcription factors independently of its protease activity [48]. Taken together, MUC1-ST macrophages appear to display a combination of MMPs and TIMPs that enable specific degradation of collagen type IV and may explain why the supernatant from MUC1-ST macrophages was so potent in our basement membrane extract *in vitro* invasion assays. It is this basement membrane degradation that has been proposed as a mechanism whereby

tumours invade; macrophages or neutrophils 'burrow' towards the tumour allowing cancer cells to escape [50] [51].

Patients with cancer are at an increased risk of developing venous thromboembolism (VTE) often known as Trousseau's syndrome [52]. Although a number of mechanisms have been suggested to modulate thrombogenesis in cancer [53], tissue factor which is the activator of coagulation *in vivo*, is elevated in the circulation of cancer patients and correlated with mortality [54]. Trousseau's syndrome is associated with mucin-producing adenocarcinomas and may be triggered by the interaction of circulating mucins with P- and L- selectin [55]. Here we show that MUC1-ST induced macrophages express factors that are associated with clotting and the secretion of tissue factor (*F3* gene) is significantly increased in MUC1-ST induced macrophages compared to M-CSF. Indeed, our functional studies show that conditioned medium from MUC1-ST macrophages induces faster clotting than medium from M-CSF macrophages.

It is additionally interesting to note that 14/18 of the upregulated protein-validated factors are associated with poor prognosis or invasion in breast cancers, when measured in serum or tissue; this suggests that cells which secrete these factors would have a negative impact on prognosis[39,41,47,49,54,56-72]. It is also of interest to note that in these studies 8/14 of these poorly prognostic factors have been seen to derive predominantly from stromal cells.

The overlap with the Gentles top genes associated with poor prognosis is also striking and it is important to note that these genes are correlated with prognosis in all cancers. As MUC1 is expressed by the vast majority of solid tumours [73], and aberrant hypersialylation is very common, it leaves open the possibility that MUC1-ST macrophages may also present in other carcinomas.

Considering the factors over-expressed by MUC1-ST macrophages, their functionality, transcriptome and location, it is highly likely these cells are pathogenic in breast cancer. Understanding the mechanism by which these cells are produced, in depth, is imperative and may lead to additional targeting opportunities. Indeed, targeting and depleting TAMs is now being evaluated as a potential therapeutic approach [6] [74,75] and reprogramming the phenotype

of TAMs by the use of HDAC inhibitors and TLR agonists is also being trialled [76,77]. However, TAMs are a heterogeneous group of cells [7,8,9] and increased knowledge of the large number of subtypes is necessary to make these targeting strategies a success. The presence of MUC1-ST TAMs in primary breast cancers, a MUC1-ST TAM signature being associated with poor prognosis and its phenotype contributing to systemic features of cancer, suggest that approaches based on targeting TAMs should include this subtype. Finally, as MUC1-ST macrophages are induced through interaction with Siglec-9 on monocytes, targeting the Siglec9/MUC1-ST interaction could effectively inhibit the production of the pro-cancer MUC1-ST induced macrophages and impact on survival [78].

Acknowledgements

We thank to Mansoor Saqi, Ulrich Kaldolsky and Rianne Wester of The National Institute for Health Research Biomedical Research Centre at Guy's and St Thomas' NHS Foundation Trust; The National Health Service Blood and Tissue Service, in particular Michael Saunders and Julie Stacey, for supplying leukocyte cones from healthy donors; Nicola O'Reilly at the Peptide Synthesis Lab at the CRICK Institute for support and lyophilisation; Katie Flaherty for co-scoring images and Toby Lawrence for helpful discussion.

Funding

This work was supported by MRC grants MR/R000026/1 and MC_PC_16048 and CRUK KHP Centre Grant

Authors' contributions

RB designed the study, conducted the experiments and contributed to the first draft of the manuscript; RG and FGF carried out experiments; DC and SK provided bioinformatics support; RM made the RNAseq libraries; NW, JO and CG supplied the breast cancer samples; IB and SP provided help with the VisoPharm; UM provided reagents: TN cultured CHO cell transfected with recombinant MUC1 in serum-free medium; JT-P and EP contributed helpful

discussion; JMB designed the study and wrote the first draft of the manuscript. All authors read the manuscript and made contributions.

Conflicts of interest.

Joy Burchell is a consultant to Palleon Pharmaceuticals. No further conflicts of interest.

Dedication.

The first author would like to dedicate this work to the memory of his mother, Lucy Beatson, who died during the course of this project.

Online Methods

Generation of MUC1 glycoforms. Recombinant MUC1-T and MUC1-ST were generated as previously described [24]. Quality control procedures include endotoxin testing (LAL), casein cleavage assay, MUC1-lectin ELISA, amino acid analysis and TGFβ1 ELISA on the products. There are additional functional endotoxin controls of a) TNFα measurement in supernatant of monocytes treated with MUC1-ST or MUC1-T for 48h, and b) assessment of readouts after inhibition of NFκB, AP1 and TLR4 pathways.

Isolation of monocytes. Leucocyte cones were ordered from the NHSBTS (National health blood and tissue service; under internal ethical approval). Cells were mixed 1:1 with PBS and layered on Ficoll-Paque (GE Healthcare; 1714402). Cells were spun at 800G for 30 minutes, with the brake off, and the PBMCs were taken from the buffy layer above the Ficoll-Paque. CD14+ cells were isolated from PBMCs using the MACS system (Miltenyi Biotech; 130-050-201. LS Columns; 130-042-401). Purity was checked using anti-CD14 antibodies (table 2) and seen to be >95%. If purity was below 95%, the cells were disposed of.

Culture of monocyte-derived macrophages. Freshly isolated monocytes, from fresh leucocyte cones, were cultured for 7 days at $1x10^6$/ml in AIM-V media (ThermoFisher; 12055091), in the presence of 50ng/ml recombinant M-CSF (replenished every 3 days; biolegend; 574804) or 25µg/ml recombinant MUC1-T or MUC1-ST unless otherwise stated in the figures. Cells were counted using a haemocytometer and viability was assessed using a viability dye (ThermoFisher; L23102) and flow cytometry. For M-CSF blocking studies, 10µg/ml αM-CSF was added every 3 days throughout the culture period. Supernatant was taken from these cells and aliquoted and stored at -20C prior to use for functional assays. Bright field images were captured using an EVOS XL Core Cell Imaging System.

Immunohistochemical staining of MUC1-ST. Protocol as described [79]. Briefly, 5µm FFPE sections were dewaxed, blocked with 20% FBS in PBS for 1 hour, before being treated in neuramindase buffer (50mM sodium acetate pH5.5) +/- neuramindase (Sigma; N2876; 10mU/section) for 1 hour at 37C. Sections were stained using the anti MUC1-T antibody (1B9) [80] for 1 hour (neat supernatant), washed twice in PBS, before a secondary (goat anti-mouse HRP; 1:100) was added for 1 hour. Sections were washed four times then stained with DAB (Agilent; K3467) and counterstained with haematoxylin. Sections were scanned using a Hammamatsu slide scanner and visualised for scoring using NDP View software (2.7.25).

Flow cytometry. $1x10^5$ cells were stained with a live/dead dye (ThermoFisher; L23102) in PBS for 10 minutes on ice in the dark, before being washed twice in FACS buffer (0.5% BSA [Sigma; 05482] in PBS + 2mM EDTA). Cells were then Fc blocked with Trustain (Biolegend;

422302) in FACS buffer for 10 minutes on ice in the dark. Cells were washed and then stained using a variety of antibodies +/- secondary reagents described in table 2, on ice for 30 minutes in the dark (if secondaries were used, cells were washed in FACS buffer before being further incubated on ice with secondary for 30 minutes). Cells were washed and either read immediately or fixed using 1% PFA in FACS buffer and read within 3 days. Cells were read using a BD Accuri C6 Plus flow cytometer, with analysis carried out using BD Accuri C6 Plus software. All cells were gated as follows a) FSC and SSC to exclude cellular debris (whilst also adjusting threshold) b) live/dead (only live cells carried forward) c) SSC-A vs SSC-H – only singlets carried forward. All MFIs were corrected against an appropriate isotype control. Intracellular flow cytometry was carried out using the intracellular fixation and permeabilization kit (ebioscience; 88-8824-00) according to manufacturer's instructions.

RNAseq library preparation. Monocytes from 3 donors were isolated. Matched M-CSF and MUC1-ST Monocyte derived macrophages were cultured as described. Cells were harvested and FACS sorted (BD FACSAria II Cell Sorter) for live cells after staining with a live/dead dye (ThermoFisher; L23102). Total RNA was isolated from the sorted live cells using the RNeasy Mini Kit (Qiagen; 74104) with DNAse treatment (Sigma; DN25). RNA was quantitated using the Qubit system and the RIN score was assessed using an Agilent bioanalyser 2100 (Agilent RNA 6000 Nano Kit). All samples in this study had RIN scores of 10. PolyA isolation and library preparation was performed using SureSelect Strand Specific RNA-Seq Library Preparation kit (G9691B) on 335ng of RNA per sample. Samples were run on the Illumina platform (HiSeq2500 Rapid) for 25 cycles.

RNAseq analysis. RNA seq analysis was performed on Partek Flow Software (https://www.partek.com/partek-flow/). All the tools with in the software was run with default settings, unless otherwise indicated. The quality of the sequencing reads was examined using FastQC (v0.11.4) (https://www.bioinformatics.babraham.ac.uk/projects/fastqc/). Raw sequencing reads (100-nt, paired-end) were trimmed using Trimgalore (v0.4.4) (https://www.bioinformatics.babraham.ac.uk/projects/trim_galore/). Traces of ribosomal DNA

and mitochondrial DNA were removed using the Bowtie2 (v2.2.5) [81]. Reads were aligned to the human reference genome GRCh38 using STAR (v2.5.3a) [82] with two pass mapping Multi-sample setting. Mapping and alignment quality were examined using FASTQC. Duplicate reads were removed using the MarkDuplicates function of the Picard tools (v2.17.11) (http://broadinstitute.github.io/picard/). Reads were annotated using the Partek E/M with GENCODE V30 (https://www.gencodegenes.org/human/). Samples were visualised and explored using unsupervised methods. All samples were clustered based on Principle Component Analysis (PCA), K-means clustering, tSNE and Hierarchical clustering. Gene counts were normalised using the Trimmed mean of M-values (TMM) and differentially expressed genes (DEG) between MUC1-ST and M-CSF treated samples were identified using Partek Differential Expression (DE) analysis tool. DEG with |fold change| >= 2 and FDR value <= 0.01 were used for pathway enrichment and gene ontology (GO) analysis. GO and pathway enrichment analysis was done using DAVID Bioinformatics Resources 6.8 (https://david.ncifcrf.gov/).

CIBERSORT analysis. The CIBERSORT R source code and the LM22 signature matrix file, which defines 22 immune cell types based on the expression levels of 547 genes, were downloaded from https://cibersort.stanford.edu/. Cell type deconvolution was carried out using the default parameters

ELISA. CXCL5 (biolegend; 440904) MMP14 (Bio-techne; DY918-05) and Tissue factor (Bio-techne; DY2339) sandwich ELISAs were performed as per manufacturer's instructions. Plates were read on a CLARIOstar instrument at 450nm, being corrected against 570nm, and analysed using MARS software and excel. For Siglec-9 blocking studies, monocytes were preincubated with αSiglec-9 antibodies or isotype control on ice for 30 minutes, washed, then incubated with recombinant MUC1-ST for 4 hours before being washed and cultured, as per Beatson et al 2016 [24].

Luminex. Choice of analytes was determined by RNAseq analysis. The Luminex kit was manufactured by Bio-techne and the assay was performed as per manufacturer's instructions.

Samples were analysed using Luminex Flexmap3D apparatus and analysis was performed using Xponent 4.0 software. For Siglec-9 blocking studies, monocytes were preincubated with αSiglec-9 antibodies or isotype control on ice for 30 minutes, washed, then incubated with recombinant MUC1-ST for 4 hours before being washed and cultured, as per Beatson et al 2016 [24].

Cell lines. T47D, MCF7 and E2J (T47D cells, transfected with C2GnT1 [28]; T47D(core 2)) cell lines were cultured in DMEM (ThermoFisher; 41966-029) + 10% FBS (ThermoFisher; 10270106) + pen/strep (Sigma; P4333) + glutamax (ThermoFisher; 35050-038). E2J cells were selected throughout in 500µg/ml G418 (Sigma; 04727878001). E2J and T47D cells have recently been glycophenotyped by mass spectrometry. For co-culture experiments cells were cultured in 24 well plates at $1x10^5$/ml the day before the assay. For neuramindase treatment, culture supernatant was removed, and cells were treated with 40mU/ml neuraminidase in PBS, or PBS as control, for 30mins at 37C, before being gently washed twice with PBS. Successful treatment was visualised by flow cytometry of treated cells; PNA staining increases. Epithelial cells plus monocytes were cultured in AIM-V media for 48 hours before supernatant was collected for protein analysis.

Isolation of neutrophils. 4ml fresh donor blood was taken (REC09/H0804/92) and mixed with 45µl of sterile 0.5M EDTA. Neutrophils were isolated from fresh donor blood using MACSexpress whole blood neutrophil isolation kit (Miltenyi; 130-104-434). Eythrocytes were lysed very gently (biolegend; 420301). Purity was assessed to be >95% using CD16, CD15 and CD66b antibodies by flow cytometry (table 2).

Migration assay. Cells were assayed in Bowden chambers with an 8µm pore size (353097). Freshly isolated neutrophils were placed in the top chamber (150µl at $1x10^6$/ml in AIMV media). 650µl of M-CSF or MUC1-ST macrophage supernatant was placed in the bottom chamber. Migrated cells were counted in the bottom chamber using a haemocytometer at indicated time points, in triplicate.

Invasion assay. Cells were assayed in Bowden chambers (353097) layered with extracellular matrix (Sigma; 126-2.5 or Biotechne; 3433-005-01) as per manufacturer's instructions (AIM-V media used to mix). Freshly isolated neutrophils or MCF7 cells were placed in the top chamber (150µl at $1x10^6$/ml in AIMV media). 650µl of M-CSF or MUC1-ST macrophage supernatant was placed in the bottom chamber. Migrated cells were counted in the bottom chamber using a haemocytometer at indicated time points, in triplicate.

Clotting assay. 50µl of human plasma (Sigma; P9523) was added to 50µl of supernatant from matched M-CSF or MUC1-ST macrophages. 50ul of rabbit thromboplastin (Sigma; 44213) was added as a positive control. 50µl of 30mM $CaCl_2$ was added and the optical density was immediately read at 405 on a CARIOstar plate reader as a measure of clotting density as per Ashour et al. [83]. Visual checks were made at the end of the assay. Reads were made every 20 seconds for 11 minutes. Data was analysed using MARS software, excel and GraphPad.

Phagocytosis assays. T47D cells were labelled with CSFE as per manufacturer's instructions (ebioscience; 65-0850-84), washed three times in media with serum, and co-cultured at a 1:1 ratio with M-CSF and MUC1-ST macrophages for 4 hours at 37C and 4C. For the dextran work, dextran-FITC (Sigma; FD40S) was added at 1mg/ml to M-CSF and MUC1-ST macrophages for 4 hours at 37C and 4C. Cells were analysed by flow cytometry for evidence of uptake. Active phagocytosis was inferred to be the difference between binding (assay at 4C) and uptake (assay at 37C).

MLR and plate bound aCD3 assays. M-CSF or MUC1-ST Monocyte derived macrophages were generated as described. Allogeneic PBMCs were stained with CFSE proliferation dye as per manufacturer's instructions and co-cultured at a 1:5 ratio (mϕ:PBMC) with monocyte derived macrophages. Cells were cultured for 4 days before being assessed for daughter populations by flow cytometry. For the αCD3 assays, 96 well flat-bottomed tissue culture plates were coated with 1µg/ml αCD3 overnight at 4C. Plates were washed with PBS, and PBMCs, pre-stained with efluor670 proliferation dye as per manufacturer's instructions, were

added along with supernatant from MUC1-ST macrophages or media alone. Cells were cultured for 4 days before being assessed for daughter populations by flow cytometry.

Ventana staining. Sections were stained for CD163 and CD68 using the Ventana Benchmark Ultra system using Ventana pre-diluted antibodies and standard CC1 with the benchmark Ultraview DAB detection kit. Positive control sections were run with every batch.

Tissue scoring: CD163, SERPINE1, CSF1 and CXCL5+CD68+ scoring. These were scored by 5 individuals using a 0-4 scoring system as follows

Score	0	1	2	3	4
Positive cells	negative	0-5%	5-20%	20-60%	60-100%

CD163 was taken forward for the Visiopharm analysis and chromogenic scoring. CD68 was included for immunofluorescent staining as the differential between background and positive staining was excellent.

MUC1-ST scoring: To provide greater scoring sensitivity for correlation analysis the product of percentage coverage (0-100) and intensity (0-5) was recorded for each case. These scores were performed by 3 individuals.

Geographical regions.

- **Nest.** Positive cells integrated within the tumour.
- **Edge of nest.** Positive cells on the edge of the tumour; from 0, i.e. touching tumour cells on the outer edge, to 200μm.
- **Stroma.** Positive cells beyond 200μm from edge of tumour.

RNAscope. RNAscope using the duplex system was carried out as per manufacturer's instructions using the manual method (Biotechne; 322430). Hs-SERPINE1 (Biotechne; 555961) and Hs-CSF1 (Biotechne; 313001-C2) probes were used.

BASEscope. BASEscope using the duplex system was carried out as per manufacturer's instructions using the manual method (Biotechne; 323810). BA-Hs-SIGLEC9-tv2-1zz-st, which binds to SIGLEC9 transcript variants 1 and 2, was designed by Bio-techne and used.

Immunofluorescent immunohistochemistry. 5μm FFPE sections were dewaxed, treated with H_2O_2 before performing antigen retrieval. Sections were boiled in citrate buffer (Sigma; C9999) for 30mins. Sections were washed in PBS Tween, then blocked 50% FBS for 1 hour. After washing, sections were probed with anti CD68 (1:100) and anti CXCL5 (1:50) for 1 hour. After further washing, sections were stained with donkey anti mouse 488 (1:1000) and donkey anti goat 557 (1:200) in 10% FBS and incubated for 1 hour. Final washes were performed, and sections were stained with DAPI for 30 seconds before being mounted (Vector Labs; H-100). Sections were scanned using an Olympus BX61VS and images were analysed using OylVIA software.

Visiopharm (digital pathology analysis software). NDP (Hammamatsu) images were analysed using VisioPharm analysis software. Briefly, images of CD163 stained slides were segmented into tumour vs non-tumour by creating an Application Protocol Package (APP) in the Visiopharm software, training the DeepLab v3 algorithm to differentiate between the tumour region of interest (ROI) vs the non-tumour. Deep learning involves neural network algorithms that use a cascade of many layers of nonlinear processing units for feature extraction and transformation with each successive layer using the output from the previous layer as input. Using deep learning for classification allows to segment abstract image structures that would be impossible to segment with a simple pixel classifier. In particular, DeepLabv3+ uses spatial pyramid pooling (ASPP) module augmented with image-level features to capture feature information on different scales. Post-processing steps were added to remove noise, calculate total area of ROI's, and create a tumour border ROI (300px thick region from tumour ROI into non-tumour ROI). Subsequently, a threshold algorithm-based APP for DAB staining was adjusted and used on the tumour images, to identify the percentage of total area in ROI's expressing CD163. This classification method is based on a custom

defined input band, the so called HDAB, which takes haematoxylin and DAB staining into consideration by having the two stains as the primary and secondary axis in the colour space coordinate system.

Interstitial fluid (ISF) collection. The method of Celis et al. [84] was followed. Briefly, fresh breast tissue, collected under ethical approval REC number 12/EE/0493, was diced into 1-3mm^3 pieces and incubated for 1 hour at 37C in 1ml of PBS. After incubation tissue was spun at 1000G for 2mins and supernatant removed and spun for a further 20mins at 4C at 5000G. Supernatant (ISF) was removed and stored at -20 for subsequent analysis.

TCGA correlations analyses. TCGA (BRCA) expression data for genes of interest were analysed and downloaded from xenabrowser.net (University of Santa Cruz).

Signature generation and application. The 9 gene signature was generated by applying the following filters to the >2 fold change RNAseq differential gene list (table 1, tab 2) and sorting on fold change. Transcripts per million threshold of 10. P value of >10^{10}. Top 9 genes taken independent of z-score.

Survival analysis. KMplot (www.kmplot.com) [85] was used to assess the prognostic impact of the MUC1-ST macrophage signature on patient disease and outcome, using the TCGA array and RNAseq datasets. The upper tertile was used to split the high and low populations and only JetSet probes were used.

Clinical data. Clinical data was collected, linked and anonymised by the King's Health Partners Tissue Bank. The use of tissue and data from King's Health Partners Cancer Biobank was approved under REC number 12/EE/0493.

Statistical Analysis. Statistical analysis was performed using GraphPad Prism software or MS excel. Appropriate group analysis tests were determined by assessing number of comparative groups, variance and whether the data was paired or not. Correlation analysis was performed using linear regression analysis (Pearson's).

1 Zhao, X. *et al.* Prognostic significance of tumor-associated macrophages in breast cancer: a meta-analysis of the literature. *Oncotarget* **8**, 30576-30586, doi:10.18632/oncotarget.15736 (2017).

2 Qian, B. Z. & Pollard, J. W. Macrophage diversity enhances tumor progression and metastasis. *Cell* **141**, 39-51, doi:10.1016/j.cell.2010.03.014 (2010).

3 Noy, R. & Pollard, J. W. Tumor-associated macrophages: from mechanisms to therapy. *Immunity* **41**, 49-61, doi:10.1016/j.immuni.2014.06.010 (2014).

4 Lin, E. Y., Nguyen, A. V., Russell, R. G. & Pollard, J. W. Colony-stimulating factor 1 promotes progression of mammary tumors to malignancy. *J Exp Med* **193**, 727-740, doi:10.1084/jem.193.6.727 (2001).

5 Ogura, M., Bridgeman, V. L. & Malanchi, I. Macrophages unlock progression of breast cancer cells experiencing matrigel-segregation in transplantation models. *Sci Rep* **7**, 11028, doi:10.1038/s41598-017-11403-w (2017).

6 Cassetta, L. & Pollard, J. W. Targeting macrophages: therapeutic approaches in cancer. *Nat Rev Drug Discov* **17**, 887-904, doi:10.1038/nrd.2018.169 (2018).

7 Kondratova, M. *et al.* A multiscale signalling network map of innate immune response in cancer reveals cell heterogeneity signatures. *Nat Commun* **10**, 4808, doi:10.1038/s41467-019-12270-x (2019).

8 Azizi, E. *et al.* Single-Cell Map of Diverse Immune Phenotypes in the Breast Tumor Microenvironment. *Cell* **174**, 1293-1308 e1236, doi:10.1016/j.cell.2018.05.060 (2018).

9 Ruffell, B., Affara, N. I. & Coussens, L. M. Differential macrophage programming in the tumor microenvironment. *Trends Immunol* **33**, 119-126, doi:10.1016/j.it.2011.12.001 (2012).

10 Kitamura, T. & Pollard, J. W. Therapeutic potential of chemokine signal inhibition for metastatic breast cancer. *Pharmacol Res* **100**, 266-270, doi:10.1016/j.phrs.2015.08.004 (2015).

11 Pinho, S. S. & Reis, C. A. Glycosylation in cancer: mechanisms and clinical implications. *Nat Rev Cancer* **15**, 540-555, doi:10.1038/nrc3982 (2015).

12 Burchell, J. M., Beatson, R., Graham, R., Taylor-Papadimitriou, J. & Tajadura-Ortega, V. O-linked mucin-type glycosylation in breast cancer. *Biochem Soc Trans* **46**, 779-788, doi:10.1042/BST20170483 (2018).

13 Sewell, R. *et al.* The ST6GalNAc-I sialyltransferase localizes throughout the Golgi and is responsible for the synthesis of the tumor-associated sialyl-Tn O-glycan in human breast cancer. *J Biol Chem* **281**, 3586-3594, doi:10.1074/jbc.M511826200 (2006).

14 Whitehouse, C. *et al.* A transfected sialyltransferase that is elevated in breast cancer and localizes to the medial/trans-Golgi apparatus inhibits the development of core-2-based O-glycans. *J Cell Biol* **137**, 1229-1241, doi:10.1083/jcb.137.6.1229 (1997).

15 Macauley, M. S., Crocker, P. R. & Paulson, J. C. Siglec-mediated regulation of immune cell function in disease. *Nat Rev Immunol* **14**, 653-666, doi:10.1038/nri3737 (2014).

16 Jandus, C. *et al.* Interactions between Siglec-7/9 receptors and ligands influence NK cell-dependent tumor immunosurveillance. *J Clin Invest* **124**, 1810-1820, doi:10.1172/JCI65899 (2014).

17 Laubli, H. *et al.* Engagement of myelomonocytic Siglecs by tumor-associated ligands modulates the innate immune response to cancer. *Proc Natl Acad Sci U S A* **111**, 14211-14216, doi:10.1073/pnas.1409580111 (2014).

18 Hudak, J. E., Canham, S. M. & Bertozzi, C. R. Glycocalyx engineering reveals a Siglec-based mechanism for NK cell immunoevasion. *Nat Chem Biol* **10**, 69-75, doi:10.1038/nchembio.1388 (2014).

19 Brown, G. D. & Crocker, P. R. Lectin Receptors Expressed on Myeloid Cells. *Microbiol Spectr* **4**, doi:10.1128/microbiolspec.MCHD-0036-2016 (2016).

20 Cassetta, L. *et al.* Human Tumor-Associated Macrophage and Monocyte Transcriptional Landscapes Reveal Cancer-Specific Reprogramming, Biomarkers, and Therapeutic Targets. *Cancer Cell* **35**, 588-602 e510, doi:10.1016/j.ccell.2019.02.009 (2019).

21 Picco, G. *et al.* Over-expression of ST3Gal-I promotes mammary tumorigenesis. *Glycobiology* **20**, 1241-1250, doi:10.1093/glycob/cwq085 (2010).

22 Mungul, A. *et al.* Sialylated core 1 based O-linked glycans enhance the growth rate of mammary carcinoma cells in MUC1 transgenic mice. *Int J Oncol* **25**, 937-943 (2004).

23 Storr, S. J. *et al.* The O-linked glycosylation of secretory/shed MUC1 from an advanced breast cancer patient's serum. *Glycobiology* **18**, 456-462, doi:10.1093/glycob/cwn022 (2008).

24 Beatson, R. *et al.* The mucin MUC1 modulates the tumor immunological microenvironment through engagement of the lectin Siglec-9. *Nat Immunol* **17**, 1273-1281, doi:10.1038/ni.3552 (2016).

25 Tanida, S. *et al.* Binding of the sialic acid-binding lectin, Siglec-9, to the membrane mucin, MUC1, induces recruitment of beta-catenin and subsequent cell growth. *J Biol Chem* **288**, 31842-31852, doi:10.1074/jbc.M113.471318 (2013).

26 Stanczak, M. A. *et al.* Self-associated molecular patterns mediate cancer immune evasion by engaging Siglecs on T cells. *J Clin Invest* **128**, 4912-4923, doi:10.1172/JCI120612 (2018).

27 Gentles, A. J. *et al.* The prognostic landscape of genes and infiltrating immune cells across human cancers. *Nat Med* **21**, 938-945, doi:10.1038/nm.3909 (2015).

28 Dalziel, M. *et al.* The relative activities of the C2GnT1 and ST3Gal-I glycosyltransferases determine O-glycan structure and expression of a tumor-associated epitope on MUC1. *J Biol Chem* **276**, 11007-11015, doi:10.1074/jbc.M006523200 (2001).

29 Coffelt, S. B. *et al.* IL-17-producing gammadelta T cells and neutrophils conspire to promote breast cancer metastasis. *Nature* **522**, 345-348, doi:10.1038/nature14282 (2015).

30 Mouchemore, K. A., Anderson, R. L. & Hamilton, J. A. Neutrophils, G-CSF and their contribution to breast cancer metastasis. *FEBS J* **285**, 665-679, doi:10.1111/febs.14206 (2018).

31 Galdiero, M. R., Varricchi, G., Loffredo, S., Mantovani, A. & Marone, G. Roles of neutrophils in cancer growth and progression. *J Leukoc Biol* **103**, 457-464, doi:10.1002/JLB.3MR0717-292R (2018).

32 Rosales, C. Neutrophil: A Cell with Many Roles in Inflammation or Several Cell Types? *Front Physiol* **9**, 113, doi:10.3389/fphys.2018.00113 (2018).

33 Kolaczkowska, E. & Kubes, P. Neutrophil recruitment and function in health and inflammation. *Nat Rev Immunol* **13**, 159-175, doi:10.1038/nri3399 (2013).

34 Lammermann, T. *et al.* Neutrophil swarms require LTB4 and integrins at sites of cell death in vivo. *Nature* **498**, 371-375, doi:10.1038/nature12175 (2013).

35 Schuster, S., Hurrell, B. & Tacchini-Cottier, F. Crosstalk between neutrophils and dendritic cells: a context-dependent process. *J Leukoc Biol* **94**, 671-675, doi:10.1189/jlb.1012540 (2013).

36 Najafi, M., Farhood, B. & Mortezaee, K. Extracellular matrix (ECM) stiffness and degradation as cancer drivers. *J Cell Biochem* **120**, 2782-2790, doi:10.1002/jcb.27681 (2019).

37 Acerbi, I. *et al.* Human breast cancer invasion and aggression correlates with ECM stiffening and immune cell infiltration. *Integr Biol (Camb)* **7**, 1120-1134, doi:10.1039/c5ib00040h (2015).

38 Khan, U. T. *et al.* Venous thromboembolism and mortality in breast cancer: cohort study with systematic review and meta-analysis. *BMC Cancer* **17**, 747, doi:10.1186/s12885-017-3719-1 (2017).

39 Georgoudaki, A. M. *et al.* Reprogramming Tumor-Associated Macrophages by Antibody Targeting Inhibits Cancer Progression and Metastasis. *Cell Rep* **15**, 2000-2011, doi:10.1016/j.celrep.2016.04.084 (2016).

40 Medrek, C., Ponten, F., Jirstrom, K. & Leandersson, K. The presence of tumor associated macrophages in tumor stroma as a prognostic marker for breast cancer patients. *BMC Cancer* **12**, 306, doi:10.1186/1471-2407-12-306 (2012).

41 Richardsen, E., Uglehus, R. D., Johnsen, S. H. & Busund, L. T. Macrophage-colony stimulating factor (CSF1) predicts breast cancer progression and mortality. *Anticancer Res* **35**, 865-874 (2015).

42 Wagner, J. *et al.* A Single-Cell Atlas of the Tumor and Immune Ecosystem of Human Breast Cancer. *Cell* **177**, 1330-1345 e1318, doi:10.1016/j.cell.2019.03.005 (2019).

43 Shiota, T. *et al.* The Clinical Significance of CD169-Positive Lymph Node Macrophage in Patients with Breast Cancer. *PLoS One* **11**, e0166680, doi:10.1371/journal.pone.0166680 (2016).

44 Wu, C. *et al.* Sialoadhesin-positive macrophages bind regulatory T cells, negatively controlling their expansion and autoimmune disease progression. *J Immunol* **182**, 6508-6516, doi:10.4049/jimmunol.0804247 (2009).

45 Ancuta, P. *et al.* CD16+ monocyte-derived macrophages activate resting T cells for HIV infection by producing CCR3 and CCR4 ligands. *J Immunol* **176**, 5760-5771, doi:10.4049/jimmunol.176.10.5760 (2006).

46 Chenivesse, C. *et al.* Pulmonary CCL18 recruits human regulatory T cells. *J Immunol* **189**, 128-137, doi:10.4049/jimmunol.1003616 (2012).

47 Chen, J. *et al.* CCL18 from tumor-associated macrophages promotes breast cancer metastasis via PITPNM3. *Cancer Cell* **19**, 541-555, doi:10.1016/j.ccr.2011.02.006 (2011).

48 Sakamoto, T. & Seiki, M. Integrated functions of membrane-type 1 matrix metalloproteinase in regulating cancer malignancy: Beyond a proteinase. *Cancer Sci* **108**, 1095-1100, doi:10.1111/cas.13231 (2017).

49 Tetu, B. *et al.* The influence of MMP-14, TIMP-2 and MMP-2 expression on breast cancer prognosis. *Breast Cancer Res* **8**, R28, doi:10.1186/bcr1503 (2006).

50 Espinoza-Sanchez, N. A., Chimal-Ramirez, G. K. & Fuentes-Panana, E. M. Analyzing the Communication Between Monocytes and Primary Breast Cancer Cells in an Extracellular Matrix Extract (ECME)-based Three-dimensional System. *J Vis Exp*, doi:10.3791/56589 (2018).

51 Huang, C. P. *et al.* Engineering microscale cellular niches for three-dimensional multicellular co-cultures. *Lab Chip* **9**, 1740-1748, doi:10.1039/b818401a (2009).

52 Shao, B. *et al.* Carcinoma mucins trigger reciprocal activation of platelets and neutrophils in a murine model of Trousseau syndrome. *Blood* **118**, 4015-4023, doi:10.1182/blood-2011-07-368514 (2011).

53 Campello, E., Henderson, M. W., Noubouossie, D. F., Simioni, P. & Key, N. S. Contact System Activation and Cancer: New Insights in the Pathophysiology of Cancer-Associated Thrombosis. *Thromb Haemost* **118**, 251-265, doi:10.1160/TH17-08-0596 (2018).

54 Hernandez, C. *et al.* Tissue factor expressed by microparticles is associated with mortality but not with thrombosis in cancer patients. *Thromb Haemost* **110**, 598-608, doi:10.1160/TH13-02-0122 (2013).

55 Wahrenbrock, M., Borsig, L., Le, D., Varki, N. & Varki, A. Selectin-mucin interactions as a probable molecular explanation for the association of Trousseau syndrome with mucinous adenocarcinomas. *J Clin Invest* **112**, 853-862, doi:10.1172/JCI18882 (2003).

56 Bieche, I. *et al.* CXC chemokines located in the 4q21 region are up-regulated in breast cancer. *Endocr Relat Cancer* **14**, 1039-1052, doi:10.1677/erc.1.01301 (2007).

57 Romero-Moreno, R. *et al.* The CXCL5/CXCR2 axis is sufficient to promote breast cancer colonization during bone metastasis. *Nat Commun* **10**, 4404, doi:10.1038/s41467-019-12108-6 (2019).

58 Hildenbrand, R. & Schaaf, A. The urokinase-system in tumor tissue stroma of the breast and breast cancer cell invasion. *Int J Oncol* **34**, 15-23 (2009).

59 Li, S. *et al.* Plasminogen activator inhibitor-1 in cancer research. *Biomed Pharmacother* **105**, 83-94, doi:10.1016/j.biopha.2018.05.119 (2018).

60 Espinoza-Sanchez, N. A., Chimal-Ramirez, G. K., Mantilla, A. & Fuentes-Panana, E. M. IL-1beta, IL-8, and Matrix Metalloproteinases-1, -2, and -10 Are Enriched upon Monocyte-Breast Cancer Cell Cocultivation in a Matrigel-Based Three-Dimensional System. *Front Immunol* **8**, 205, doi:10.3389/fimmu.2017.00205 (2017).

61 Zou, A. *et al.* Elevated CXCL1 expression in breast cancer stroma predicts poor prognosis and is inversely associated with expression of TGF-beta signaling proteins. *BMC Cancer* **14**, 781, doi:10.1186/1471-2407-14-781 (2014).

62 Wang, J., He, Q., Shao, Y. G. & Ji, M. Chemokines fluctuate in the progression of primary breast cancer. *Eur Rev Med Pharmacol Sci* **17**, 596-608 (2013).

63 Wang, D. *et al.* Clinical Significance of Elevated S100A8 Expression in Breast Cancer Patients. *Front Oncol* **8**, 496, doi:10.3389/fonc.2018.00496 (2018).

64 Zhang, S. *et al.* Distinct prognostic values of S100 mRNA expression in breast cancer. *Sci Rep* **7**, 39786, doi:10.1038/srep39786 (2017).

65 Kim, H., Watkinson, J., Varadan, V. & Anastassiou, D. Multi-cancer computational analysis reveals invasion-associated variant of desmoplastic reaction involving INHBA, THBS2 and COL11A1. *BMC Med Genomics* **3**, 51, doi:10.1186/1755-8794-3-51 (2010).

66 Barcus, C. E. *et al.* Elevated collagen-I augments tumor progressive signals, intravasation and metastasis of prolactin-induced estrogen receptor alpha positive mammary tumor cells. *Breast Cancer Res* **19**, 9, doi:10.1186/s13058-017-0801-1 (2017).

67 Liu, K. L., Fan, J. H. & Wu, J. Prognostic Role of Circulating Soluble uPAR in Various Cancers: a Systematic Review and Meta-Analysis. *Clin Lab* **63**, 871-880, doi:10.7754/Clin.Lab.2017.170110 (2017).

68 Bae, Y. K. *et al.* Fibronectin expression in carcinoma cells correlates with tumor aggressiveness and poor clinical outcome in patients with invasive breast cancer. *Hum Pathol* **44**, 2028-2037, doi:10.1016/j.humpath.2013.03.006 (2013).

69 Ruelland, A., Kerbrat, P., Clerc, C., Legras, B. & Cloarec, L. Level of plasma fibronectin in patients with breast cancer. *Clin Chim Acta* **178**, 283-287, doi:10.1016/0009-8981(88)90236-7 (1988).

70 Wei, L. *et al.* High Indoleamine 2,3-Dioxygenase Is Correlated With Microvessel Density and Worse Prognosis in Breast Cancer. *Front Immunol* **9**, 724, doi:10.3389/fimmu.2018.00724 (2018).

71 Ager, E. I. *et al.* Blockade of MMP14 activity in murine breast carcinomas: implications for macrophages, vessels, and radiotherapy. *J Natl Cancer Inst* **107**, doi:10.1093/jnci/djv017 (2015).

72 Ueno, T., Toi, M., Koike, M., Nakamura, S. & Tominaga, T. Tissue factor expression in breast cancer tissues: its correlation with prognosis and plasma concentration. *Br J Cancer* **83**, 164-170, doi:10.1054/bjoc.2000.1272 (2000).

73 Xu, F., Liu, F., Zhao, H., An, G. & Feng, G. Prognostic Significance of Mucin Antigen MUC1 in Various Human Epithelial Cancers: A Meta-Analysis. *Medicine (Baltimore)* **94**, e2286, doi:10.1097/MD.0000000000002286 (2015).

74 Papadopoulos, K. P. *et al.* First-in-Human Study of AMG 820, a Monoclonal Anti-Colony-Stimulating Factor 1 Receptor Antibody, in Patients with Advanced Solid Tumors. *Clin Cancer Res* **23**, 5703-5710, doi:10.1158/1078-0432.CCR-16-3261 (2017).

75 Mantovani, A., Marchesi, F., Malesci, A., Laghi, L. & Allavena, P. Tumour-associated macrophages as treatment targets in oncology. *Nat Rev Clin Oncol* **14**, 399-416, doi:10.1038/nrclinonc.2016.217 (2017).

76 Guerriero, J. L. *et al.* Class IIa HDAC inhibition reduces breast tumours and metastases through anti-tumour macrophages. *Nature* **543**, 428-432, doi:10.1038/nature21409 (2017).

77 Wang, J. *et al.* Effect of TLR agonists on the differentiation and function of human monocytic myeloid-derived suppressor cells. *J Immunol* **194**, 4215-4221, doi:10.4049/jimmunol.1402004 (2015).

78 Tomioka, Y. *et al.* A soluble form of Siglec-9 provides an antitumor benefit against mammary tumor cells expressing MUC1 in transgenic mice. *Biochem Biophys Res Commun* **450**, 532-537, doi:10.1016/j.bbrc.2014.06.009 (2014).

79 Beatson, R. *et al.* The Breast Cancer-Associated Glycoforms of MUC1, MUC1-Tn and sialyl-Tn, Are Expressed in COSMC Wild-Type Cells and Bind the C-Type Lectin MGL. *PLoS One* **10**, e0125994, doi:10.1371/journal.pone.0125994 (2015).

80 Tarp, M. A. *et al.* Identification of a novel cancer-specific immunodominant glycopeptide epitope in the MUC1 tandem repeat. *Glycobiology* **17**, 197-209, doi:10.1093/glycob/cwl061 (2007).

81 Langmead, B. & Salzberg, S. L. Fast gapped-read alignment with Bowtie 2. *Nat Methods* **9**, 357-359, doi:10.1038/nmeth.1923 (2012).

82 Dobin, A. *et al.* STAR: ultrafast universal RNA-seq aligner. *Bioinformatics* **29**, 15-21, doi:10.1093/bioinformatics/bts635 (2013).

83 Ashour, M. B., Gee, S. J. & Hammock, B. D. Use of a 96-well microplate reader for measuring routine enzyme activities. *Anal Biochem* **166**, 353-360, doi:10.1016/0003-2697(87)90585-9 (1987).

84 Celis, J. E. *et al.* Proteomic characterization of the interstitial fluid perfusing the breast tumor microenvironment: a novel resource for biomarker and therapeutic target discovery. *Mol Cell Proteomics* **3**, 327-344, doi:10.1074/mcp.M400009-MCP200 (2004).

85 Nagy, A., Lanczky, A., Menyhart, O. & Gyorffy, B. Validation of miRNA prognostic power in hepatocellular carcinoma using expression data of independent datasets. *Sci Rep* **8**, 9227, doi:10.1038/s41598-018-27521-y (2018).

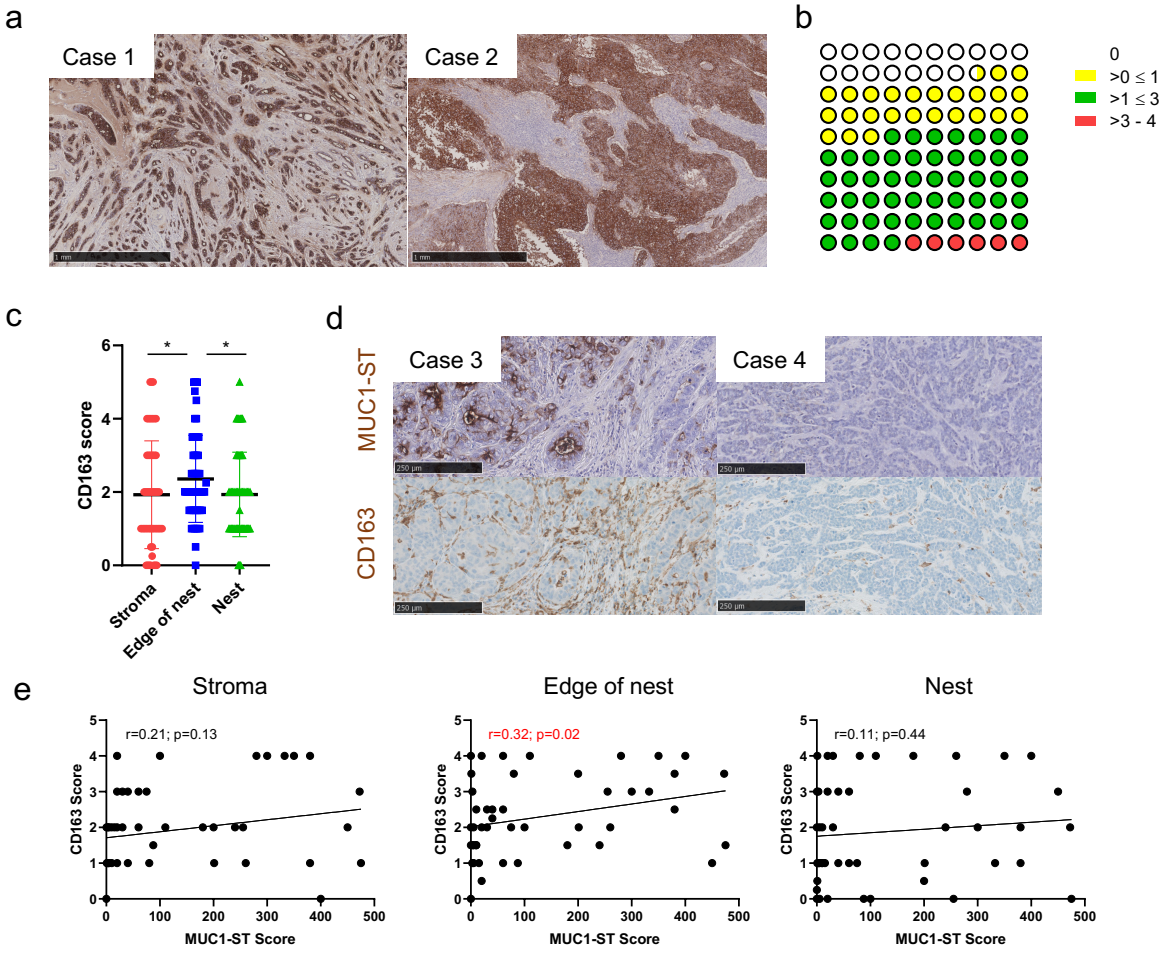

Figure 1. MUC1-ST is expressed by most breast cancers and its expression positively correlates with macrophage presence on the edge of tumour nests **(a)** Examples of positive MUC1-ST IHC staining in breast cancers. **(b)** Summary of tissue scoring of MUC1-ST expression in breast cancers (n=53). **(c)** CD163 scores in different regions of breast cancers (n=53) **(d)** Examples of sequential sections stained for MUC1-ST (brown) and CD163 (brown) by IHC **(e)** CD163 scores in different indicated regions of the tumour measured against MUC1-ST scoring (n=53). Standard error of the mean shown and paired t-test used for statistical analysis *p=<0.05. Correlations were analysed using linear regression analysis (Pearson's).

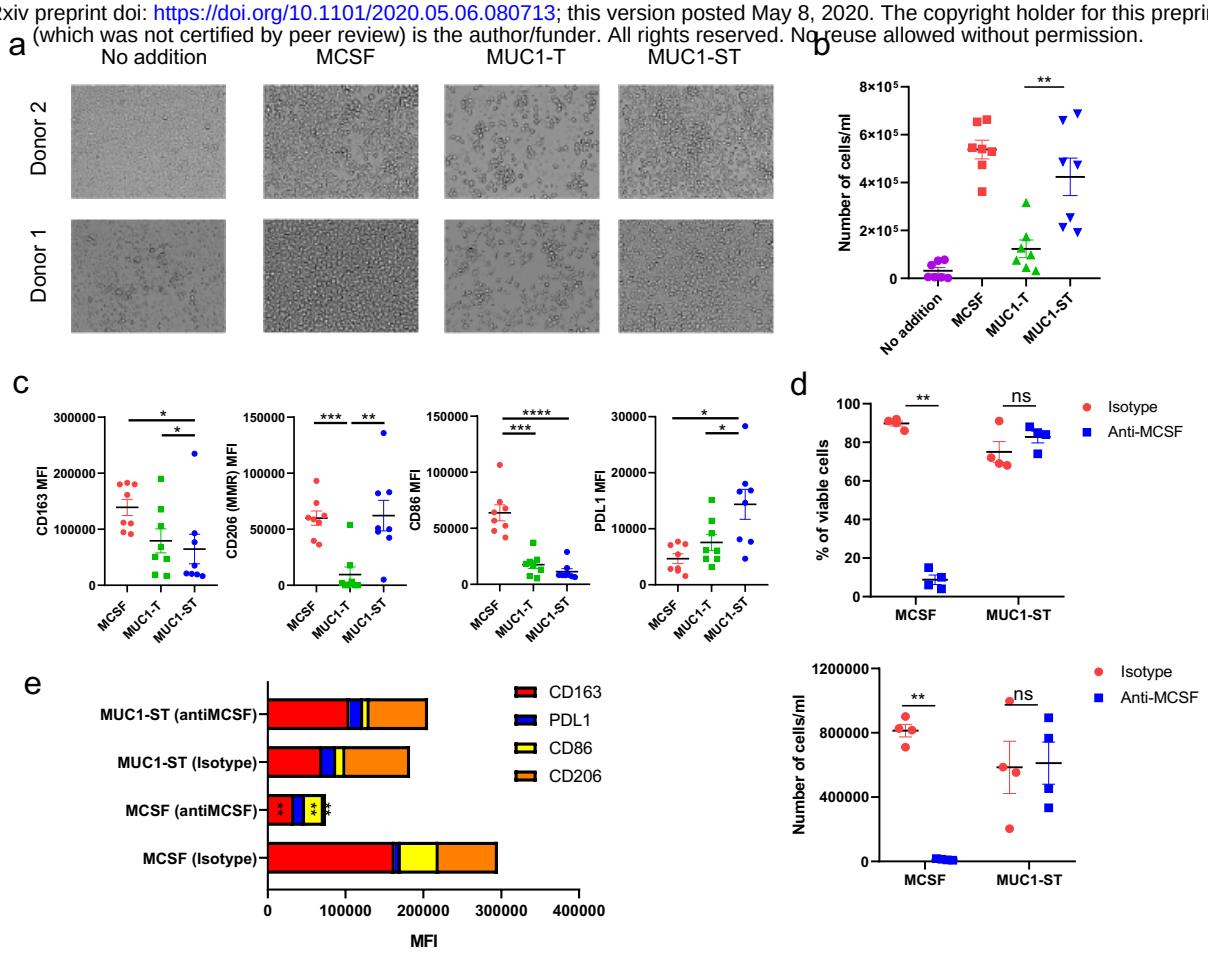

Figure 2. Recombinant MUC1-ST can induce the differentiation of monocytes into TAMs in an M-CSF independent manner. **(a)** Bright field images of representative healthy donor monocytes treated with indicated factors for 7 days in serum-free media **(b)** Number of viable cells from monocytes treated with indicated factors for 7 days in serum-free media (n=7) **(c)** Phenotype of monocytes treated with indicated factors for 7 days in serum-free media (n=8) **(d)** Number and viability of monocytes cultured with either MCSF or MUC1-ST for 7 days in serum-free media in the presence of anti-MCSF neutralising antibodies or isotype control (n=4) **(e)** summary of phenotype for cells in (d). Standard error of mean shown and paired t-test used for statistical analysis. * p<0.05 **p<0.01 ***p<0.001 ****p<0.0001

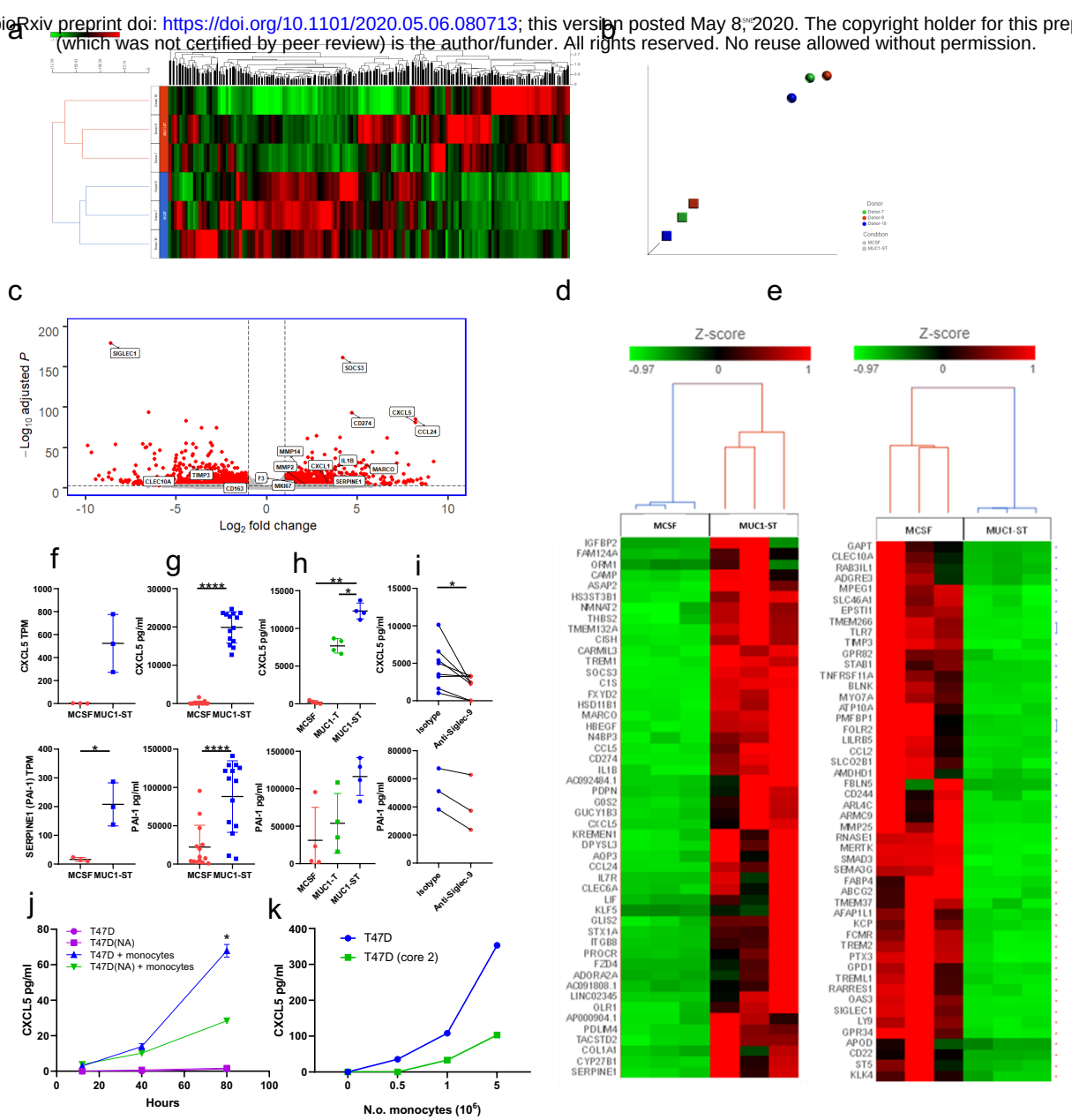

Figure 3. MUC1-ST induced a novel TAM phenotype. **(a)** Hierarchical clustering of all transcripts from matched MUC1-ST (n=3) and MCSF (n=3) treated monocytes after RNAseq and Partek flow analysis. **(b)** t-sne plot showing clustering of MUC1-ST and MCSF treated monocyte transcriptomes (n=3). **(c)** Volcano plot showing the fold change and significance (FDR) of differentially expressed genes in matched MUC1-ST and MCSF macrophages (n=3). Low expressed genes removed (see supplementary table 1; tab 3) **(d)** Top 50 differentially expressed genes between matched MUC1-ST and MCSF macrophages. Low expressed genes removed (see supplementary table 1; tab 3) **(e)** As (d) but bottom 50 expressed genes. **(f,g,h,i)** Top row CXCL5, bottom row SERPINE1/PAI-1. Validation of two of the top hits, CXCL5 and SERPINE1/PAI-1. **(f)** CXCL5 and SERPINE1 transcript expression in matched monocytes treated with MCSF (n=3) or MUC1-ST (n=3) for 7 days in serum-free media. **(g)** CXCL5 and PAI-1 protein levels in the supernatant of monocytes treated with MUC1-ST or MCSF for 7 days in serum-free media (n=14). **(h)** CXCL5 and PAI-1 levels in the supernatant of monocytes treated with MUC1-ST or desialylated MUC1-ST (MUC1-T) for 7 days in serum-free media (n=4). **(i)** CXCL5 (n=8) and PAI-1 (n=3) levels in the supernatant of MUC1-ST macrophages pre-treated with anti-Siglec-9 antibodies or isotype control. **(j)** CXCL5 levels in the supernatant of monocyte/T47D (+/- neuraminidase pretreatment; NA) cocultures after 48h of co-culture at a 5:1 ratio, n=2, technical triplicate. **(k)** CXCL5 levels in the supernatant of monocyte/T47D or monocyte/T47D (core 2) cocultures after 48h of co-culture at a 5:1 ratio. Representative of 2 independent experiments. Standard error of mean shown and paired t-test used for statistical analysis *p<0.05, **p<0.01, ****p<0.0001. TPM; Transcripts per million.

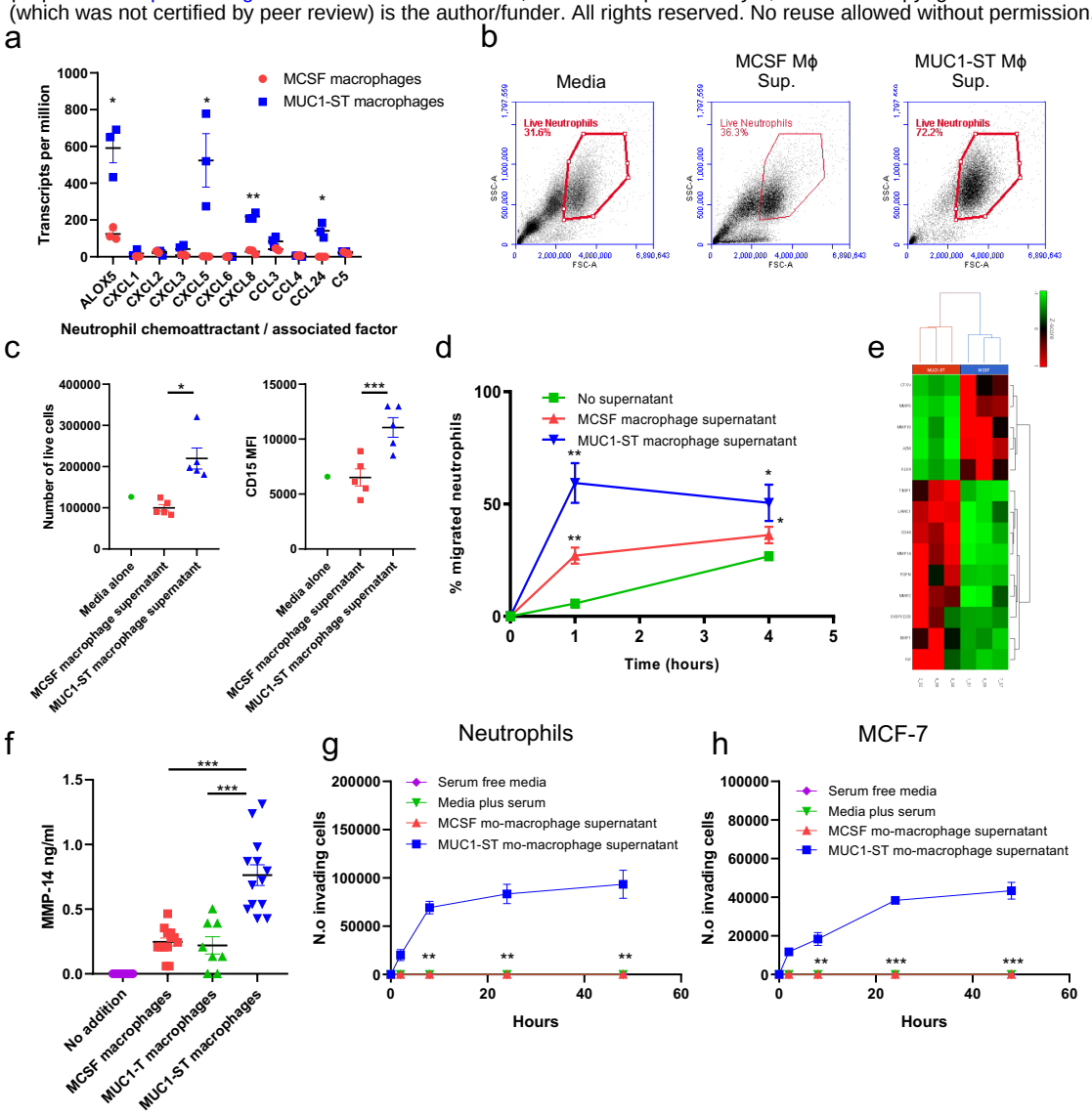

Figure 4. MUC1-ST macrophages can sustain neutrophils and induce their migration and invasion. **(a)** Neutrophil chemoattractant or associated factor transcript expression level in MUC1-ST macrophages (n=3) and MCSF macrophages (n=3). **(b)** Example FSC/SSC plots of live neutrophils 48h after being cultured in indicated media or supernatant (n=5). **(c)** Numbers and phenotype of neutrophils 48h after being cultured in indicated media or supernatant (n=5). **(d)** Migration of neutrophils towards indicated media or supernatant over indicated time period (n=5). **(e)** Heatmap showing differentially expressed extracellular matrix disassembly genes (GO:0022617) in MUC1-ST (n=3) and MCSF (n=3) macrophages. **(f)** MMP14 protein levels in supernatant of monocytes treated with indicated factors for 7 days (n=13; desialylated MUC1-ST, MUC1-T, n=8). **(g)** Number of neutrophils invading through basement membrane extract towards the indicated media or supernatant at the indicated time points (n=5). **(h)** Number of breast cancer cells (MCF-7) invading through basement membrane extract towards the indicated media or supernatant at the indicated time points (n=5). Standard error of mean shown and paired t-test used for statistical analysis *p<0.05, **p<0.01, ***p<0.001.

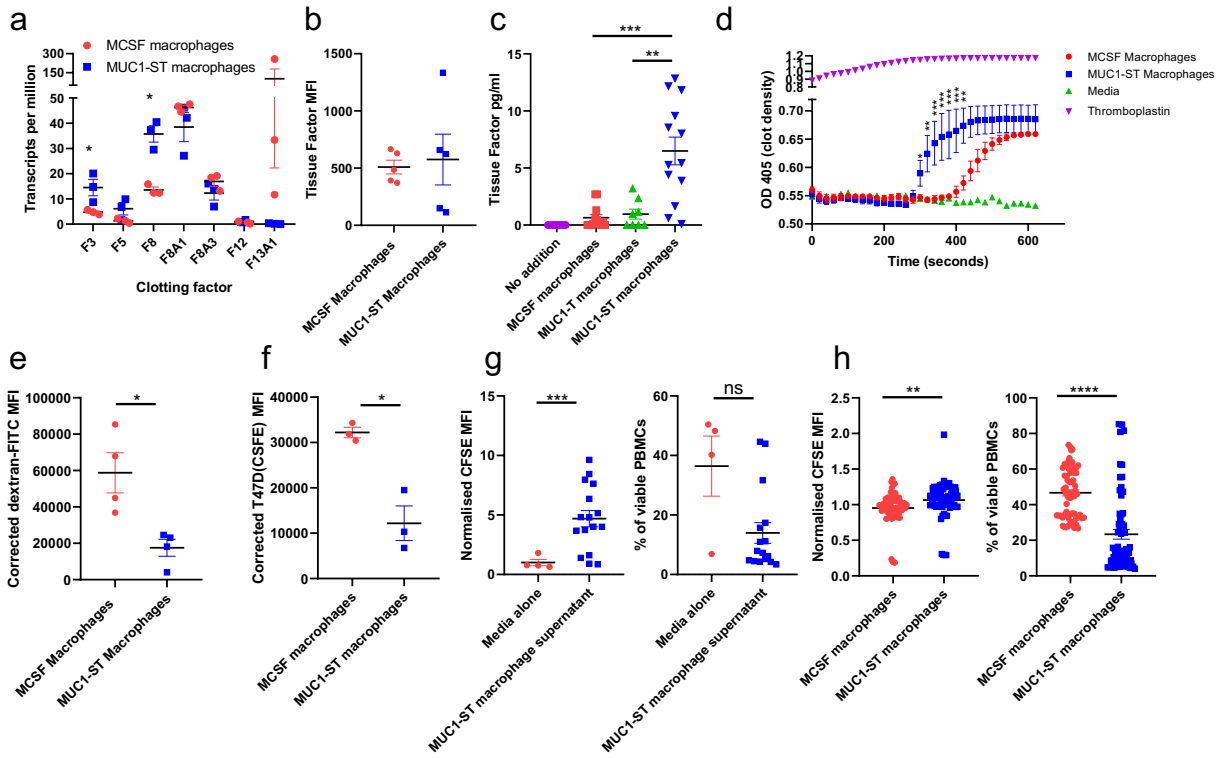

Figure 5. MUC1-ST macrophages induce clotting, are inefficient at phagocytosis and inhibit T cell proliferation and viability. **(a)** Clotting factor transcript expression levels in MUC1-ST (n=3) and MCSF macrophages (n=3). **(b)** Cell surface bound (n=5) and **(c)** secreted levels of tissue factor (n=13); excluding MUC1-T where n=8. **(d)** Plasma clotting in the presence of indicated factors or supernatants at indicated time points. **(e-f)** Bar charts showing corrected (37ºC MFI minus 4ºC MFI) of **(e)** dextran-FITC uptake, n=4 and **(f)** uptake of CFSE labelled T47D tumour cells, n=3 by M-CSF macrophages and MUC1-ST macrophages after 4h incubation. **(g)** Pooled data showing proliferation (relative CFSE expression) and viability of CD3 stimulated PBMCs in the presence of media alone (n=4) or MUC1-ST macrophage supernatant (n=16). **(h)** Mixed leukocyte reaction showing proliferation and viability of PBMCs when co-cultured with MCSF macrophages or MUC1-ST macrophages at a 5:1 ratio for 4 days (n=64). Standard error of the mean shown and paired t-test used for statistical analysis *p<0.05, **p<0.01, ***p<0.001, ****p<0.0001.

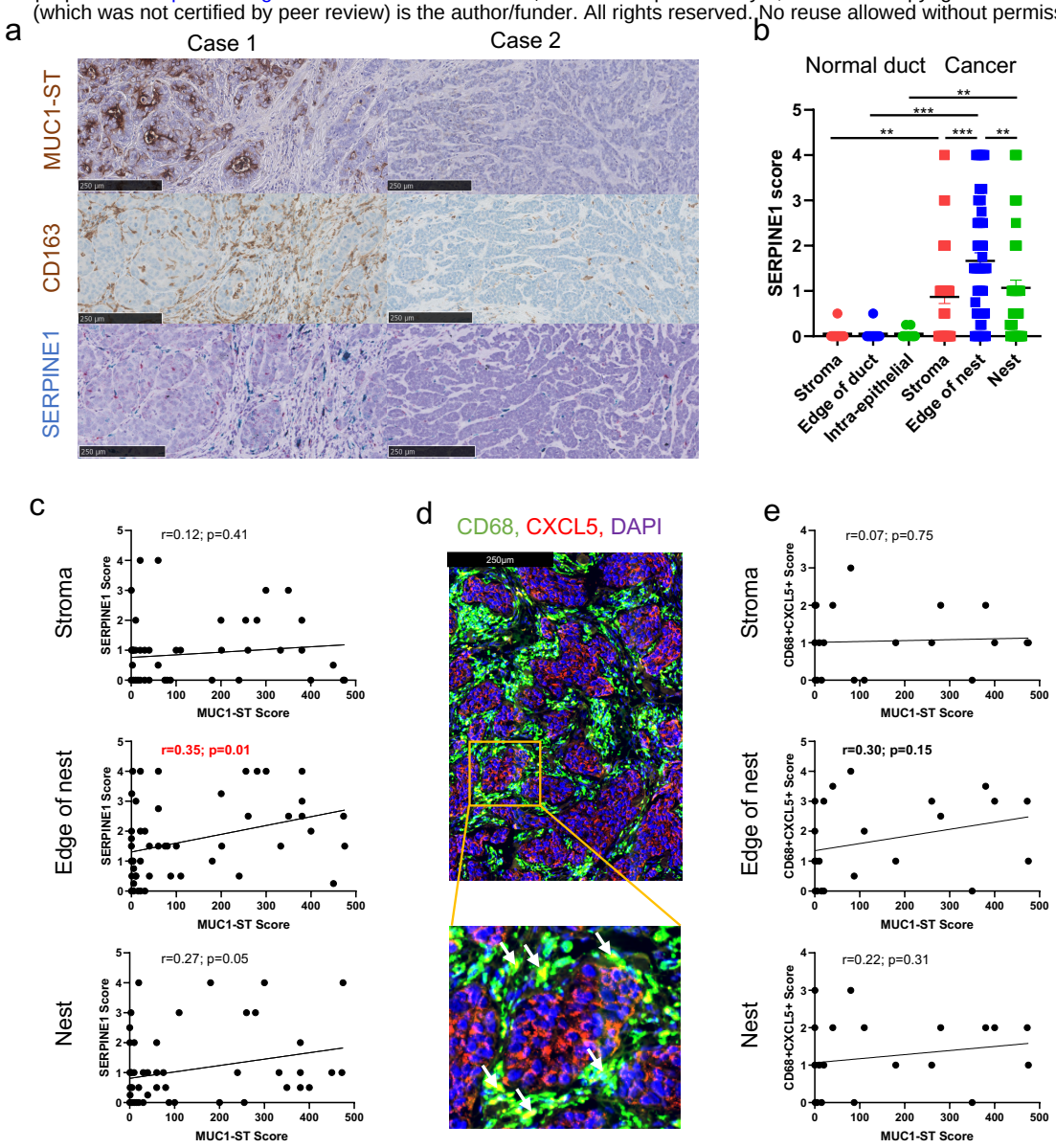

Figure 6. MUC1-ST macrophages are present in the stroma surrounding primary breast cancers. **(a)** Sequential sections stained for MUC1-ST (brown) and CD163 (brown) by IHC and *SERPINE1* (blue/green) by RNAscope. **(b)** Scoring of *SERPINE1 expression* in different indicated regions of healthy ducts (n=12) and tumours (n=53). **(c)** *SERPINE1* scores in different indicated regions of the tumour measured against MUC1-ST scoring (n=53). **(d)** Example image of CD68+CXCL5+ double staining; double positive cells are displayed as yellow as indicated by arrows. **(e)** *CD68+CXCL5+* scores in different indicated regions of the tumour measured against MUC1-ST scoring (n=24) Standard error of the mean shown and paired t-test used for statistical analysis **p=<0.01, ***p=<0.001. Correlations were analysed using linear regression analysis (Pearson's).

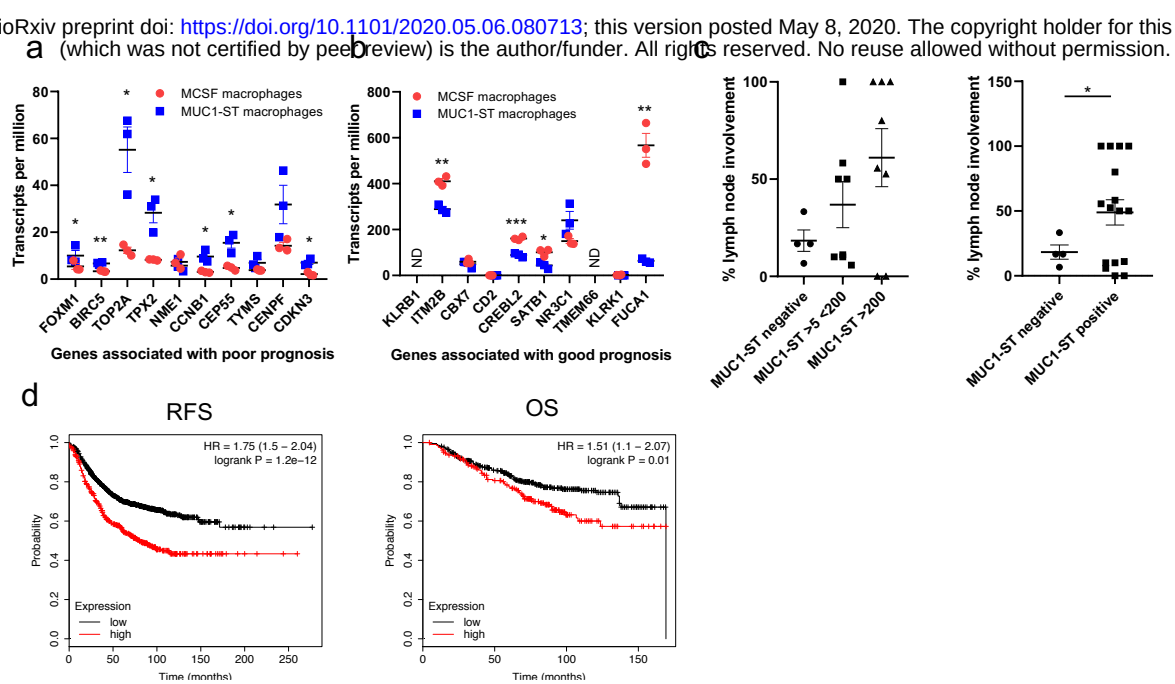

Figure 7. MUC1-ST differentially expressed genes are associated with poor clinical outcome. **(a)** Top 10 genes associated with a poor prognosis or **(b)** good prognosis (described in Gentles et al. [27]), expressed by MUC1-ST macrophages (n=3) or MCSF macrophages (n=3) **(c)** Percentage of lymph nodes positive for cancer in relation to their primary cancer MUC1-ST score (n=20). **(d)** A 9 gene signature was derived from top genes (fold change) from the differential expression analysis of MCSF macrophages and MUC1-ST macrophages (fold change >2, p value >1^{10}), and was applied to the BRCA TCGA database. RFS, relapse free survival; OS, overall survival; ND, not detected. Standard errors of the mean shown. (a-b) *p<0.05 **p<0.01 ***p<0.001 using paired t-test. (c) *p<0.05 using unpaired t-test with Welch's correction owing to unequal population variance.